wjert, 2021, Vol. 7, Issue 6, 148-174. *Original Article* ISSN 2454-695X

World Journal of Engineering Research and Technology

WJERT

www.wjert.org

SJIF Impact Factor: 5.924

INVESTIGATION FOR VARIATION OF PERFORMANCE OF A HEXAGONAL CENTRIFUGAL GOVERNOR CONTROL SYSTEM WITH ITS TREFOILS

Debarupam Gogoi[1]*, Angshumala Kashyap[2], Manasi Saikia[3], Monti Rajkhowa[4] and Sevika Sarmah[5]

[1]Assistant Professor Department of Mechanical Engineering Jorhat Engineering College, Jorhat-785007 Assam, India.

[1,2,3,4,5]All are affiliated to Jorhat Engineering College, Jorhat, India.

Article Received on 22/09/2021 **Article Revised on 12/10/2021** **Article Accepted on 02/11/2021**

***Corresponding Author**
Debarupam Gogoi
Assistant Professor
Department of Mechanical Engineering Jorhat Engineering College, Jorhat-785007 Assam, India.

ABSTRACT

A mechanical centrifugal governor has application in maintaining constant speed of a turbine shaft in power plant or in automobile by fuel control. A set of experimental case studies has been carried out by plotting characteristics curve for performance analysis of a hexagonal fuel control system with its three categories namely Porter, Proell and Hartnell governor at various load conditions to find the efficient one. The reference universal governor was set as Porter, Proell and Hartnell and interpretation were studied at three different randomly selected sleeve loads 2.765 kg, 3.265 kg and 3.765 kg to affect the controlling force. At each different stage of sleeve load, the governor was run at a set of different speeds and corresponding sleeve displacements were recorded. Then from empirical formulas for governor, other parameters such as radius of rotation, height, controlling force, effort, power, and sensitivity were calculated and characteristics curves were plotted for sleeve displacement versus governor speed and controlling force, controlling force versus radius of rotation, speed versus height to check the variations. Performances were observed from controlling force curve, effort, power, and sensitivity plot. It had been observed that at lower sleeve load Porter governor is suitable and at higher sleeve load Hartnell governor is suitable as its sensitivity is more than the other two types subjected to same set of sleeve loads.

KEYWORDS: Controlling force; Hartnell; Porter; Proell; sensitivity.

1. INTRODUCTION

A governor is a mechanical device that is used for regulating the mean speed of an engine or rather to regulate the flow of working fluid into the engine. Though it is obsolete, it is a unique mechanical feedback system that works to control the throttle action, with the variation in load on the engine. Objective of this paper is to do experimental performance analysis of a hexagonal centrifugal governor at different randomly selected sleeve loads and speed by plotting characteristic curves to figure out the suitable one. Parnaby and Porter (1968) analysed a spring controlled centrifugal governor subjected to harmonic variations which yields non-linear equations of motions and compared with previously obtained linearized equations. They also investigated harmonic and sub-harmonic content various possible vibrations. Kogiso and Hirata (2009) proposed a reference governor model for constrained linear system of time varying reference. They achieved satisfactory effectiveness by applying multi-parametric programming technique and demonstrated with numerical and experimental examples. Nakada et al. (2016) proposed a reference governor on the air path system of a diesel engine. They established an algorithm on the basis of system identification and using a real engine, they demonstrated the effectiveness of the method with experimental results. J. WANG, H. Wang, and Guo (2012) developed chaos anti-control strategy for controlling stable periodic orbit of non-autonomous system to chaotic orbit in which they derived dynamical equations and state equation of mechanical centrifugal governor through Lagrange equations. Mello, Sotomayor, and Braga (2006) studied the Lyapunov stability and Hopf bifurcation in a system which coupled Watt-centrifugal-governor with steam-engine. In addition, periodic motion and bifurcation conditions of a SDF (Single Degree of Freedom) oscillator system can be achieved from study of Cheng and Xu (2007). Ge et al. (1999) studied dynamic behavior of a rotational machine with centrifugal governor subjected to two different external disturbances. They obtained conditions of stability of the equilibrium points by applying Lyapunov direct method. They observed Hopf bifurcation in the system. They succeeded to obtain steady state responses of the three-dimensional non-autonomous system. An analogy of kinematic bifurcation and equilibrium bifurcation in stability theory of structures and mechanism is referred as presented by Lengyel and You (2006). Miljic and Popovic (2014) studied a mathematical model which deals impact of adjustable governor parameters on both dynamic and static characteristics of its variable speed in DPA distributor type fuel injection pump. Yunpu and Yixing (2014) investigated on vibration of centrifugal

block of the centrifugal over speed governor by performing simulation analysis on influence of parameters such as mass, speed, and radius to get their specific influence relationship. Manhotra (2017) eliminated the problem of hunting and dipping with the prototype which was tested in engine and used new design of plunger type stopper cover with compressed coil spring for engine rpm adjustment assembly for mechanical centrifugal fly-ball governor system. Navathale, Paralkar, and Ghorade (2017) investigated the most susceptible areas of failure when the governor is in running condition. Here they considered the weight of the arms in their analysis. They also did stress analysis of the structure and suggested materials for replacement. Rao et al. (2017) studied two-dimensional parameter space forms under nonlinear response of a centrifugal mechanical governor. They used three kinds of phases to describe the responses and found a new type of mixed mode oscillations in periodic response. Rao et al. (2018) in their study expanded the dynamical behaviors of a centrifugal hexagonal governor with a spring attachment. They used phase diagram to identify the complex mode-locking behaviors with changing parameters. Ge and Lee (2005) studied five methods for chaos synchronization and proposed two procedures to anti-control a hexagonal centrifugal governor with rotational machine system effectively. Jorge Sotomayor, Mello, and Braga (2008) studied a system coupling steam engine with centrifugal governor under Lyapunov stability and Hopf bifurcation. Sensitivity of a shape varying structure like governor plays important rule. In this project, Hartnell governor is found to be more sensitive than other two. Sensitivity analysis of this kind may be referred from Dems and Haftka (2007).

1. MATERIALS AND METHODS

The procedure while doing the experiments can be summarised with a flow diagram as shown in Figure 1.

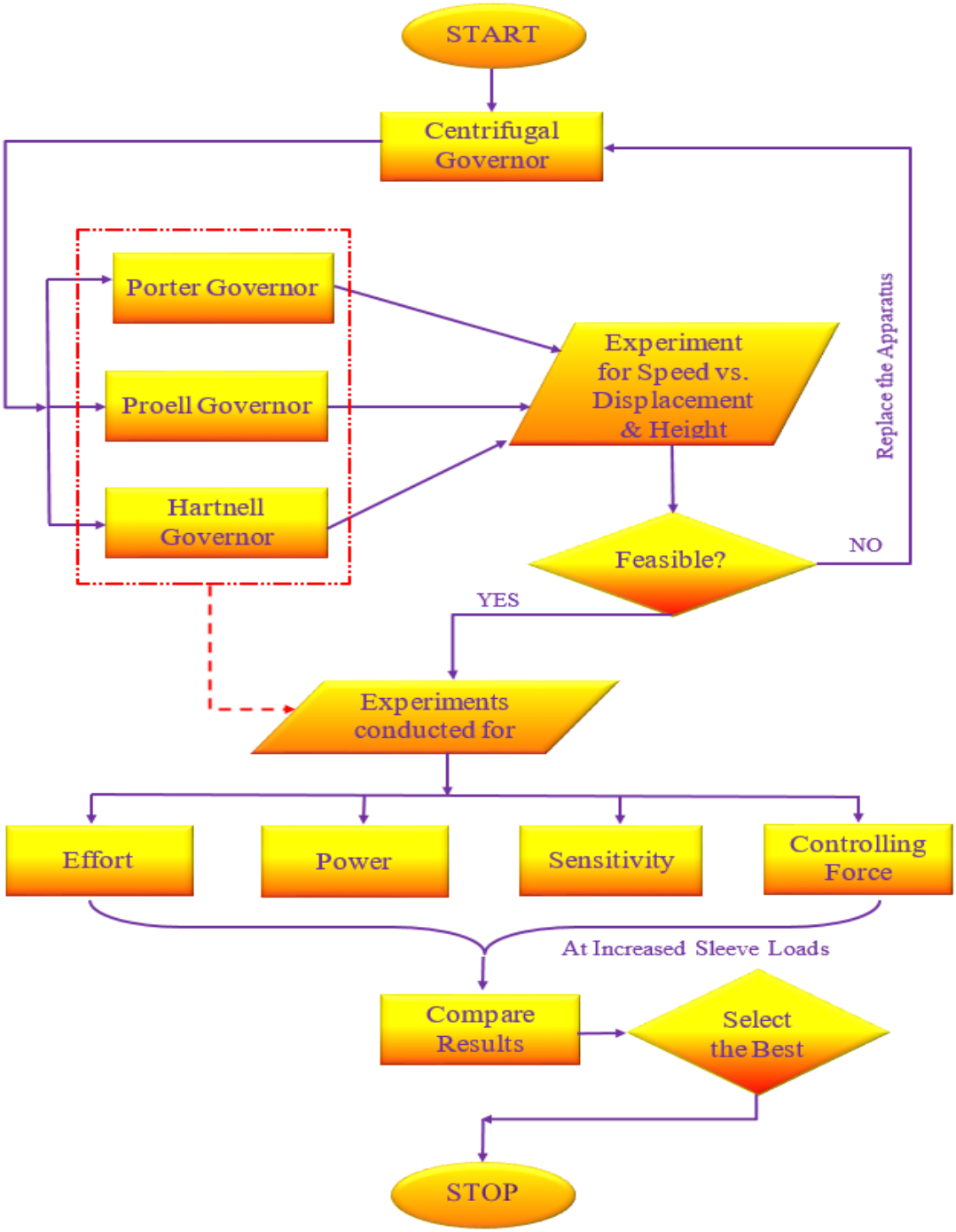

Figure 1: Flow diagram showing methods of experiment on the three governors.

In Porter governor, the fly-ball connects the upper and lower links which are connected with the spindle at pivot point and sleeve respectively or may offset as shown in Fig. 2. Unlike Porter governor, the fly-balls are extended vertically by small links from the junction of upper and lower link. Porter and Proell governors are dead weight loaded type governor, where controlling force (equivalent to centripetal force) is provided by weight of fly-ball and sleeve.

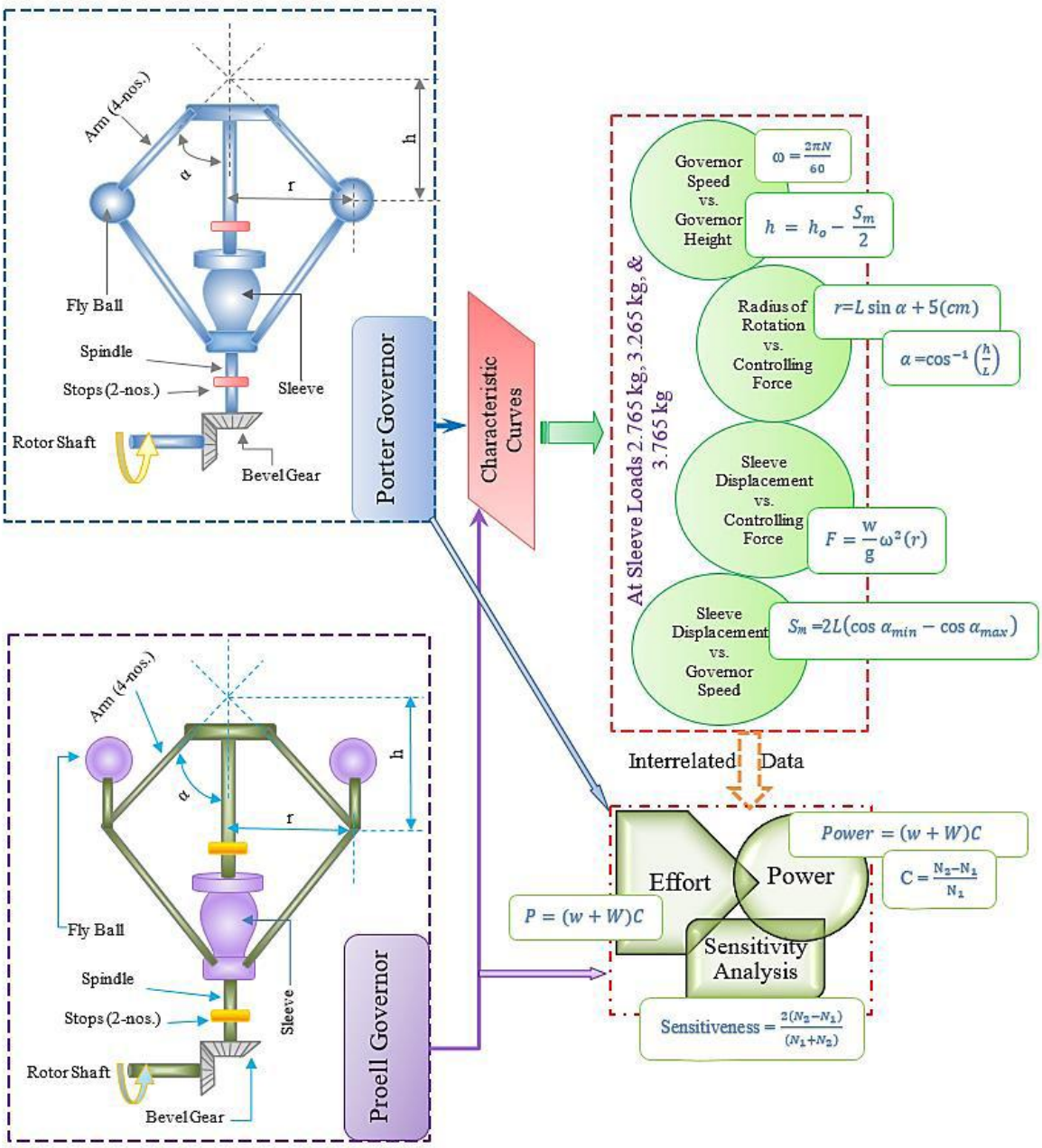

Figure 2: Schematic of Porter and Proell Governor and Experiments done for.

On the other hand, Hartnell governor is incorporated with a spring on the spindle as shown in Fig. 3. It is a spring-controlled governor as the controlling force is mainly provided by the spring force.

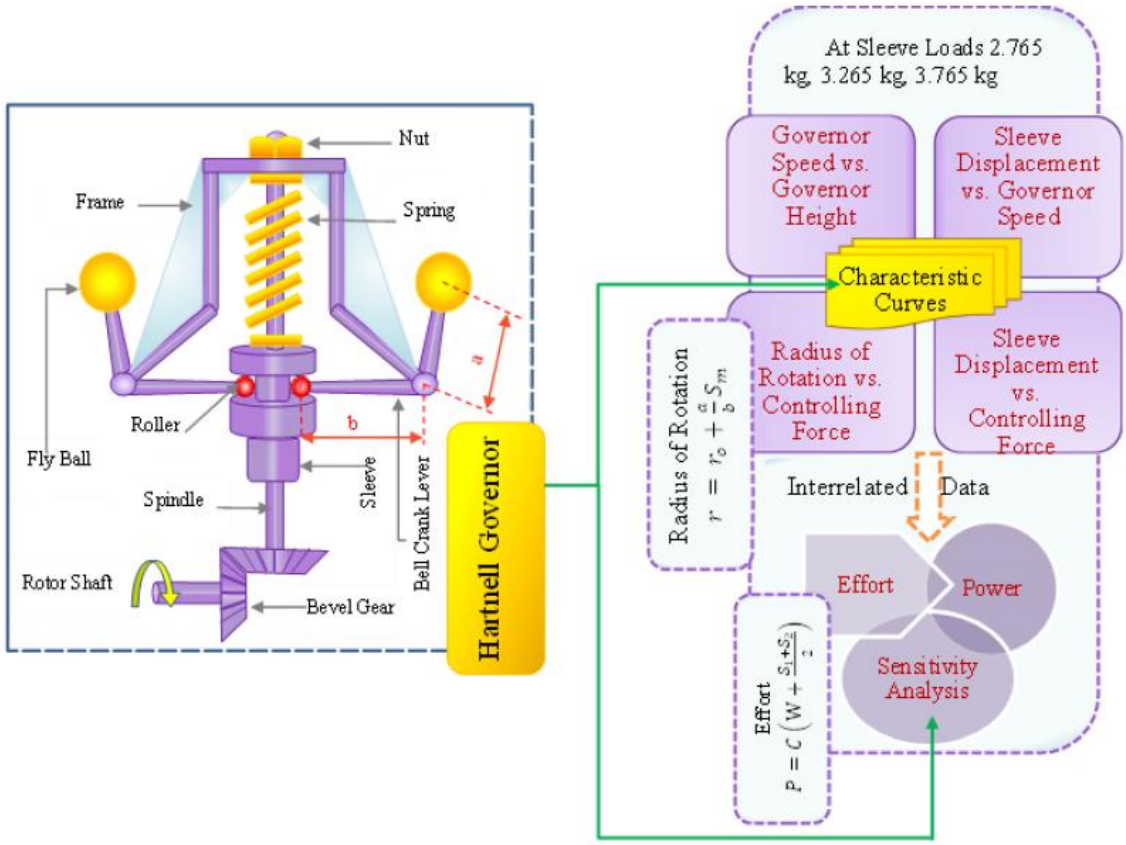

Figure 3: Hartnell Governor and Experiments done for.

The magnitude of the controlling of governor is a measure of the force that can be exerted at the sleeve to operate the control mechanism. The area under the controlling force curve for minimum radius (r_{min}) and maximum radius (r_{max}) of operation represents the work done by the governor against the resultant of all external forces, i.e., controlling force. This also represents the energy released by the fly balls when the speed falls from maximum to minimum radius position. The total energy capacity of the governor is expressed as:

$E = 2\int_{r_{min}}^{r_{max}} F dr = 2\int_{r_{min}}^{r_{max}} F(r) dr$, Where $F(r) = m(\omega)^2 r$ (1)

$= 2\int_{\alpha_{min}}^{\alpha_{max}} (m+M) L g \tan(\alpha) \cos\alpha d\alpha$

$= 2(m+M) L g \int_{\alpha_{min}}^{\alpha_{max}} (\sin\alpha) d\alpha$

$= (m+M) 2L(\cos\alpha_{min} - \cos\alpha_{max}) g$

$= (m+M) g \times S_m$, [$S_m = 2L(\cos\alpha_{min} - \cos\alpha_{max})$](2)

Here, $\tan\alpha = \frac{\sin\alpha}{\cos\alpha} = \frac{r}{h}$,(3)

where *'r'* is radius of rotation and *'h'* is the height of governor with mass of the fly ball '*m*', sleeve mass '*M*' and arm length '*L*'.

From Eq. 1, $(\omega)^2 = \frac{F(r)}{m \times r}$

=> $(N)^2 = \frac{(m+M)}{m} \times \frac{895}{h}$,

(4) Equation (4) is applicable when angle of inclination of upper and lower arms are equal and having same length of upper and lower arms neglecting friction. For Proell governor, the expression for governor speed with similar condition becomes

$$(N)^2 = \frac{a}{e}\frac{(m+M)}{m} \times \frac{895}{h} \quad (5)$$

where 'a/e' is a fraction less than one. Again, height *'h'* of the Porter governor from above equation can be expressed as:

$$h = \frac{g}{(\omega)^2} + \frac{Mg(1+k)}{2m(\omega)^2} = \frac{2mg+Mg(1+k)}{2m(\omega)^2} \quad (6)$$

where $k = \frac{\tan\beta}{\tan\alpha}$(7)

$'\beta'$ is angle of inclination of lower arm with spindle axis. Now, if ω be increased by '*c*' times

ω where *c* is the percentage change in speed and *E* be the mean force applied on the sleeve to prevent it from moving so that forces on the sleeve is increased to (*Mg* + *E*), then

$$h = \frac{2mg + (Mg+E)(1+K)}{2m(1+c)^2(\omega)^2} \quad (8)$$

From Eq. (6) and (8) (Rattan 2011)

$$\frac{2mg + (Mg+E)(1+k)}{2mg+Mg(1+k)} = \frac{(1+c)^2}{1}$$

Or, $\frac{[2mg + (Mg+E)(1+k)] - [2mg+Mg(1+k)]}{2mg+Mg(1+k)} = \frac{1+(c)^2+2c-1}{1}$

Or, $\frac{E(1+k)}{2mg\ Mg(1+k)} = 2c$

Or, $E = \frac{2c}{(1+k)}[2mg + Mg(1+k)]$

Or, $E/2 = \frac{cg}{(1+k)}[2m + M(1+k)]$(9)

In our case, as upper arms and lower arms are of equal length and offset by 5cm from the spindle axis. So, from Eq. (7), $\alpha = \beta$ and hence $k = 1$ and Eq. (9) becomes

$P = (m + M)\ cg$(10)

And Power = Effort × Sleeve displacement

2.1 Porter Governor Set-up

To determine the four characteristic curves for the porter governor, viz. i) sleeve displacement vs. governor speed ii) sleeve displacement vs. controlling force iii) Radius of rotation vs. controlling force iv) height vs. speed, the universal governor was set as a porter governor as shown in Fig. 2 with each link length 15cm, weight of each fly ball 0.35kg, initial radius of rotation and height 15 cm each. Making proper connection of the 0.25HP, 1500 RPM, 230Volts, 1Amp motor, the speed of motor is slowly and gradually increased. The speed of the spindle is measured by a tachometer and the sleeve displacement is obtained from scale reading. As controlling force is dependent on sleeve loads mainly, three different sets of readings are taken for sleeve weights 2.765kg, 3.265kg and 3.765 kg. Figure 2 shows the experimental setup of Universal Governor as Porter, Proell and Figure 3 shows that of Hartnell governor.

As the arms and links are of equal length (each 15cm) and offset by 5 cm from spindle axis, so angle of inclination of upper arm and lower arm are equal to each other so that, governor height, h (Khurmi and Gupta 2005) is expressed as:

$$h = h_o - \frac{S_m}{2} \quad (11)$$

Where 'h_o' is initial height of governor and 'S_m' is the displacement or lift of sleeve.

Angle of inclination of upper link (Thomas 2009):

$\alpha = \cos^{-1}\left(\frac{h}{L}\right)$(12)

Radius of rotation (Rao and Dukkipati 2014):

$r = L \sin\alpha + 5$ (cm)(13)

As upper links are offset by 5cm from spindle axis in the model. Controlling Force (Ghosh and Mallik 2004; Bansal and Brar 2015):

$F = \frac{w}{g}\omega^2(r)$(14)

For 2.765kg load, at nine different speeds from 240 rpm to 330 rpm sleeve displacements were observed and found to vary from 2.2 cm to 9.5 cm. Again for 3.265 kg sleeve load, at eight different rpm speed; ranging from 230 rpm to 330 rpm; eight readings of sleeve displacements up to 8.6 cm were observed. And finally; for 3.765 kg load; seven different spindle speeds in rpm which ranges in between 250 rpm to 320 yield 1.3 to 6.7 cm sleeve displacements as listed in Table 1.

Table 1: Sleeve Displacement and Controlling forces of porter governor at different sleeve Weight and Speed.

	Sl No.	Speed, N (rpm)	Sleeve Displacement (S_m) (cm)	Governor Height ($h=S_m-x/2$) (cm)	$\alpha=\cos^{-1}\left(\frac{h}{L}\right)$ (degree)	$r=L\sin\alpha+5$ (Cm)	Controlling Force $F=\frac{w}{g}\omega^2(r)$ (Newton)
For Weight, W= 2.765kg	1	240	2.2	13.9	22.1	10.64	18.94
	2	245	3.1	13.45	26.28	11.64	21.59
	3	250	4.1	12.95	30.31	12.57	24.28
	4	265	5	12.5	33.56	13.29	28.84
	5	280	6.1	11.95	37.19	14.07	34.09
	6	290	6.9	11.55	39.65	14.57	37.87
	7	295	7.4	11.3	41.12	14.86	39.97
	8	310	8.6	10.7	44.5	15.51	46.07
	9	330	9.5	10.25	46.89	15.95	53.68
For weight, W= 3.265kg							
	1	230	1	14.5	14.84	8.84	17.06
	2	255	3	13.5	25.84	11.54	27.51
	3	270	3.4	13.3	27.54	11.94	31.76
	4	280	4.6	12.7	32.15	12.98	37.14
	5	290	5.8	12.1	36.23	13.86	42.54
	6	300	6.9	11.55	39.65	14.57	47.86
	7	310	8.0	11	42.83	15.2	53.31

	8	330	8.6	10.7	44.5	15.51	61.64
For weight, $W=3.765kg$							
	1	250	1.3	14.35	16.93	9.37	23.25
	2	260	1.9	14.05	20.5	10.25	29.16
	3	270	2.3	13.85	22.58	10.76	33.01
	4	280	3.5	13.25	27.95	12.03	39.69
	5	290	4.7	12.65	32.51	13.06	46.22
	6	310	6.5	11.75	38.43	14.32	57.91
	7	320	6.7	11.65	39.04	14.44	62.23

Figure 4(a) proves that with increase in governor speed, height falls and Fig. 4(b) shows speed vs. height, sleeve lift, angle of inclination of upper arm, radius of rotation, and controlling force for 2.765kg sleeve load of Porter governor.

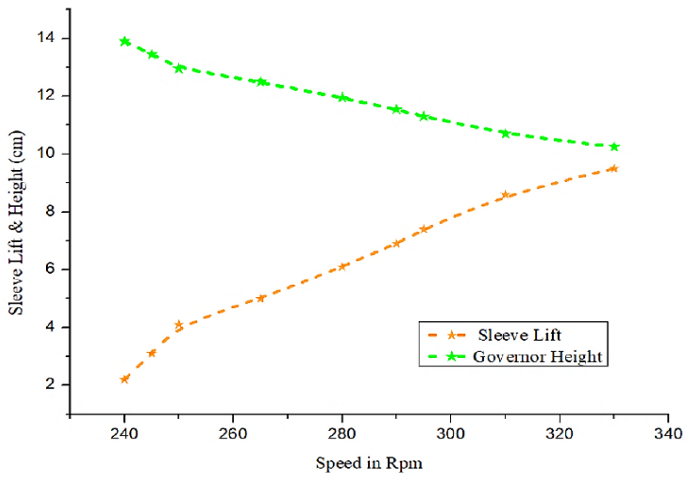

Figure 4(a): Governor Speed versus Sleeve Displacement and Height Plot.

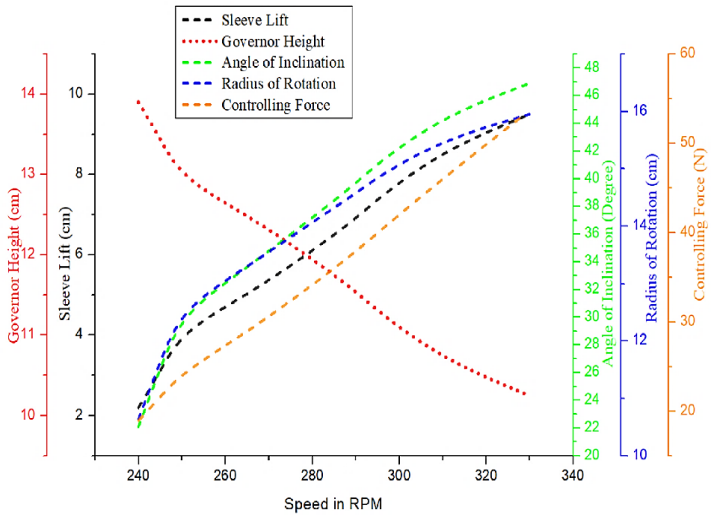

Figure 4(b): Governor Speed versus Height, Sleeve Lift, Angle of Inclination, Radius of Rotation, Controlling Force Plot.

The four characteristics curves for the mentioned three different sleeve loads; 2.765 kg, 3.265 kg and 3.765 kg, were obtained from the results are shown in Fig. 5. (To reduce the number of drawings with space, Radar Chart is preferred in graphical representation)

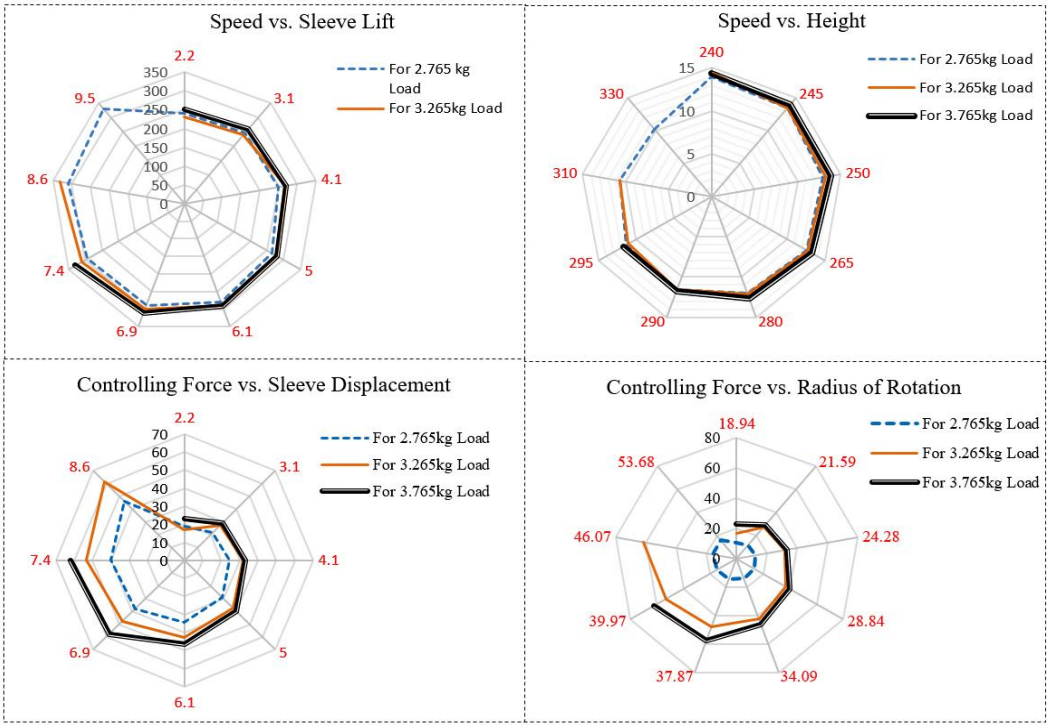

Figure 5: Plot of Speed versus i) Sleeve Lift, ii) Height and Controlling Force versus i) Sleeve Lift, ii) Radius of Rotation.

As per Eq. (2), the energy of the Porter governor at three load conditions against speed is plotted in Fig. 6. So, energy capacity increases with increase in speed. The governor will release this energy when speed falls from maximum to minimum. Area under each curve represents the work done by the governor against total external force acting on the system.

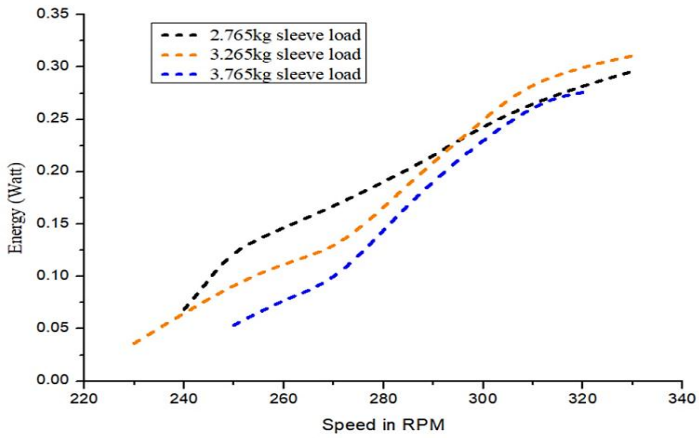

Figure 6: Energy versus speed plot of porter governor.

The controlling force curve of Porter governor may be drawn by taking radius of rotation in abscissa and controlling force in primary ordinate and speed in rpm in secondary ordinate. Figure 7 shows the controlling force curve for 2.765 kg, 3.265 kg and 3.765 kg sleeve load.

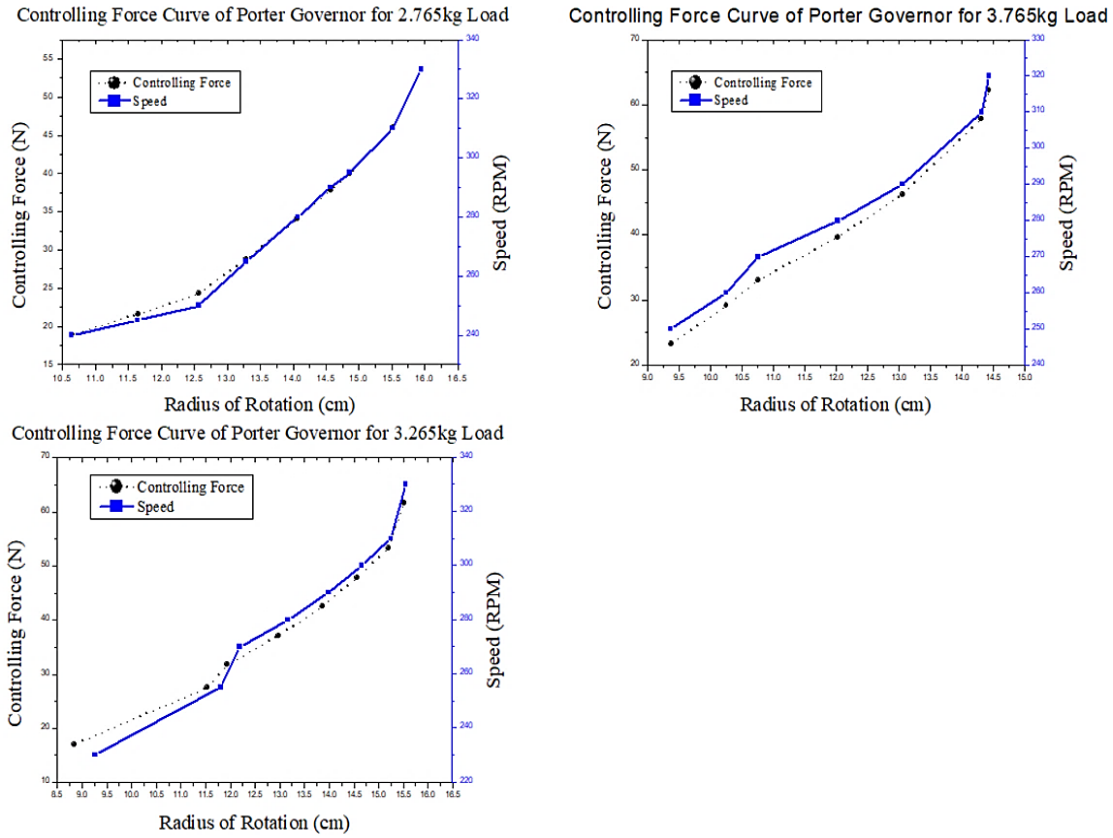

Figure 7: Controlling force curve of porter governor for 2.765 kg, 3.265 kg and 3.765 kg Sleeve Load.

2.2 Proell Governor Set-up

For plotting the characteristic curves of Proell governor the universal governor was set up accordingly as shown in Fig. 2 in which length of link, L=12.4cm; initial height of governor, h_o=10cm; initial radius of rotation, r_o = 13cm and weight of each fly ball, w = 0.35kg. After making proper connection with the motor, the speed of motor is gradually increased and speed of spindle is measured with a tachometer and sleeve displacement by the scale provided for three different loads given to the sleeve.

For 2.765 kg load, eight different speeds were selected which lies in between 85 rpm to 220 rpm and as a result, obtained sleeve displacements are from 0.01 to 3.2 cm. With 3.265 kg load, sleeve lifts of 0 to 3.67 cm are noticed for eight different speeds from 125 rpm to 175

rpm. Similarly, 0 to 6.6 cm sleeve displacements are observed for spindle speed from 160 rpm to 195 rpm as listed in Table 2.

Table 2: Sleeve Displacement and Controlling forces of proell governor at different sleeve Weight and Speed.

	Sl No.	Speed, *N* (rpm)	Sleeve displacement (S_m) (cm)	Governor height ($h=ho-S_m/2$) (cm)	$\alpha = \cos^{-1}\left(\frac{h}{L}\right)$ (degree)	$r = L\sin\alpha + 5$ (cm)	Controlling force $F = \frac{w}{g}\omega^2(r)$ (Newton)
For weight, *W*= 2.765kg	1	85	0.01	9.995	36.28	12.33	2.75
	2	100	0.09	9.955	36.59	12.39	3.83
	3	140	0.56	9.72	38.38	12.69	7.68
	4	165	1.2	9.40	40.70	13.08	11.00
	5	175	1.9	9.05	43.12	13.47	12.75
	6	200	2.4	8.80	44.79	13.73	16.97
	7	210	2.9	8.55	46.40	13.97	19.04
	8	220	3.2	8.40	47.35	14.12	21.12
For weight , *W*= 3.265kg							
	1	125	0	10.0	36.24	12.33	7.03
	2	145	0.10	9.95	36.63	12.39	9.5
	3	150	0.70	9.65	38.90	12.78	10.49
	4	155	1.00	9.50	39.99	12.96	11.36
	5	160	1.75	9.125	42.61	13.39	12.51
	6	165	2.43	8.785	44.88	13.74	13.65
	7	170	3.00	8.50	46.72	14.02	14.78
	8	175	3.67	8.165	48.81	14.33	16.01
For weight, *W*= 3.765kg							
	1	160	0	9.995	36.28	12.33	13.28
	2	165	0.9	9.55	39.63	12.90	14.78
	3	170	2.2	8.90	44.13	13.63	16.57
	4	175	3.4	8.30	47.98	14.21	18.31
	5	180	4.3	7.85	50.72	14.59	19.89
	6	185	4.8	7.60	52.2	14.79	21.3
	7	190	5.5	7.40	53.36	14.94	22.69
	8	195	6.6	6.70	57.29	15.43	24.69

Figure 8(a) proves the correctness of the system set-up by establishing that with increase in speed, sleeve lift increases and height of governor falls.

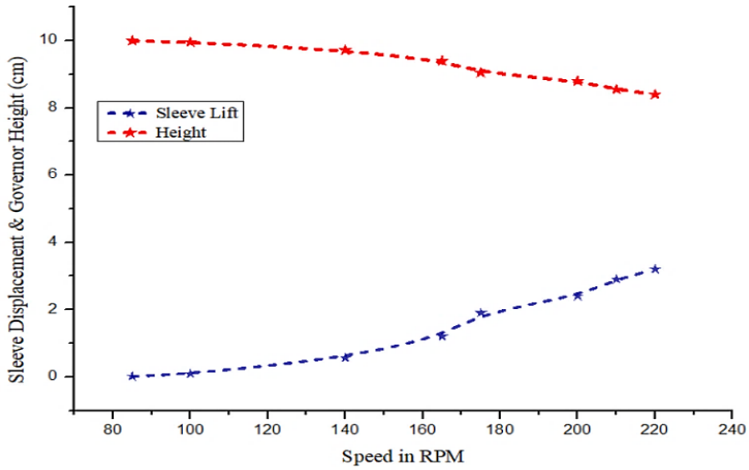

Figure 8(a): Speed versus Sleeve Lift and Height Plot.

From Fig. 4(a) and Fig. 8(a), it is obvious that Proell governor can be applicable for higher speeds as compared to Porter governor. Plot of Governor Height, Sleeve displacement, Angle of Inclination of upper arm, Radius of rotation and Controlling force against Governor speed has been shown in Fig. 8(b).

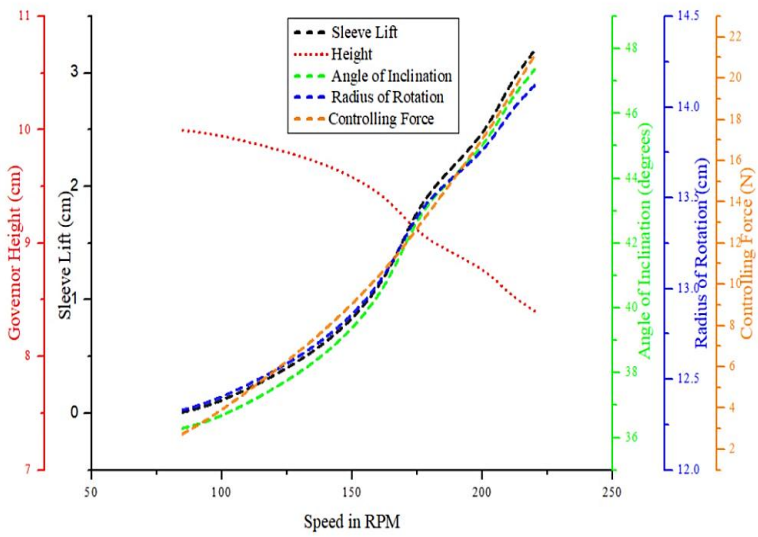

Figure 8(b): Height, Sleeve lift, Angle of inclination, Radius of rotation, Controlling force versus Governor speed.

Figure 9 shows the four characteristic curves for sleeve loads 2.765 kg, 3.265 kg and 3.765 kg loads. (Radar chart is preferred for convenience)

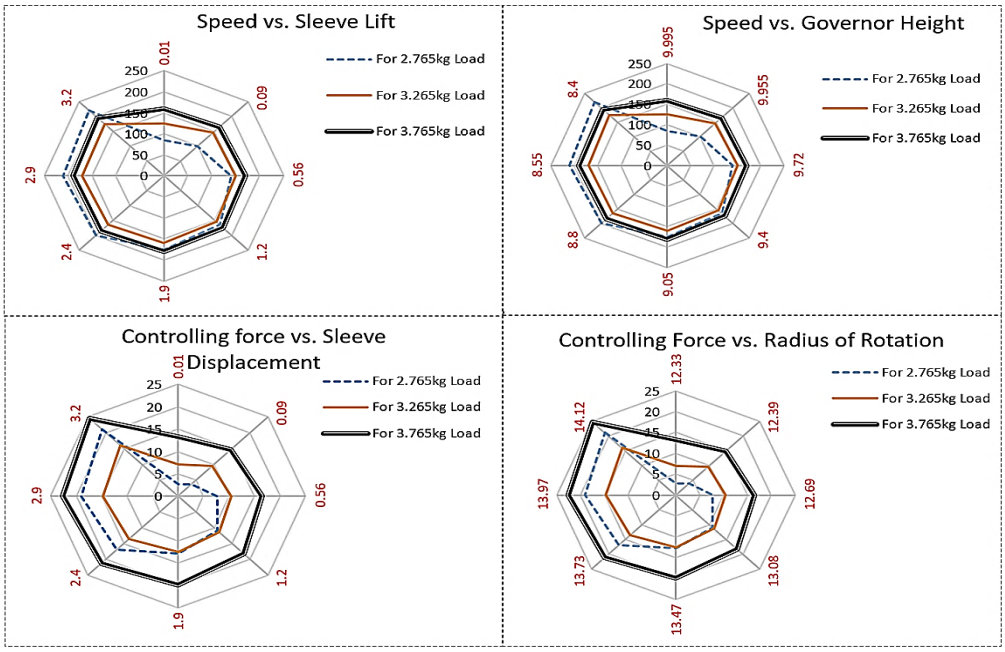

Figure 9: Plot of Speed versus i) Sleeve lift ii) Governor height and Controlling force versus i) Sleeve lift ii) Radius of rotation.

The controlling force curve of Proell governor may be drawn by taking radius of rotation in abscissa and controlling force in primary ordinate and speed in rpm in secondary ordinate. Figure 10 shows the controlling force curve for 2.765 kg, 3.265 kg and 3.765 kg sleeve load.

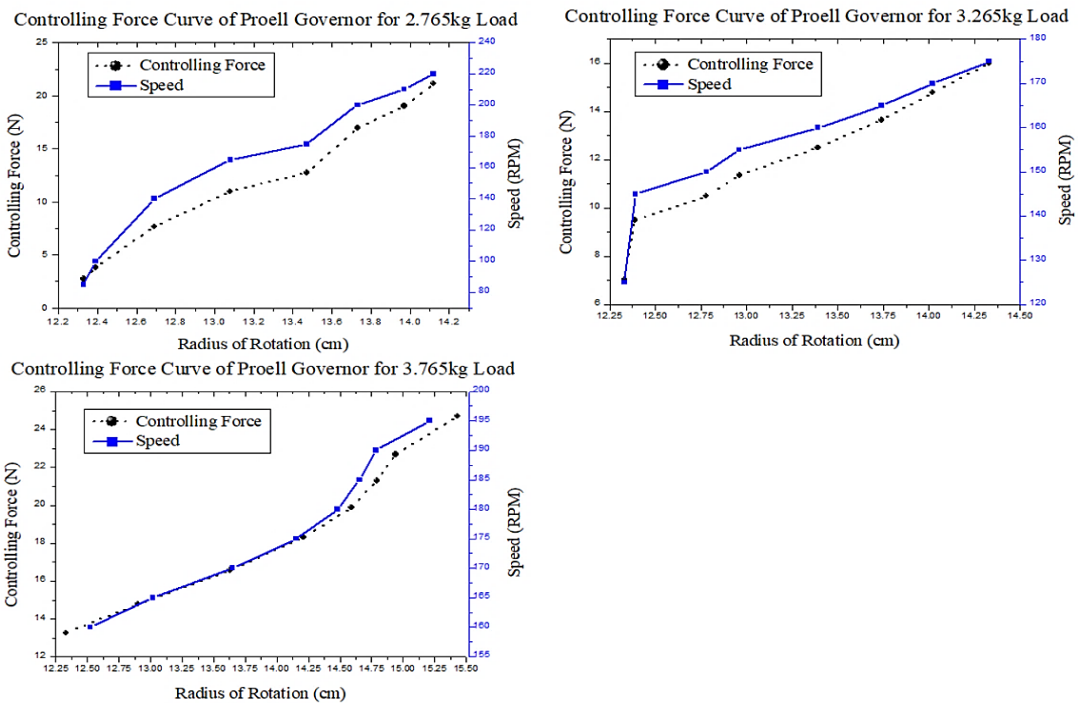

Figure 10: Controlling Force Curve of Proell Governor for 2.765 kg, 3.265 kg and 3.765 kg Sleeve Load.

To get the plot of Percentage change in speed versus Effort and Power, for an increase of sleeve load from 2.765kg to 3.265kg and then to 3.765kg, Table 3 is prepared

****Table 3: Effort and Power of Proell Governor against percentage change in speed.**

Sl. No	Weight of Sleeve, W (kg)	Initial Speed, N_1 (rpm)	Final Speed, N_2 (rpm)	Percentage change in speed $C=\frac{N_2-N_1}{N_1}$	Lift of Sleeve, S_m (cm)	Effort = $C(w + W)$	Power = Effort × Sleeve Lift
1	2.765	240	280	0.166	3.9	0.52	2.03
2		280	310	0.107	2.5	0.33	0.83
3		310	330	0.064	0.9	0.20	0.18
4	3.265	200	230	0.150	1.0	0.54	0.54
5		230	270	0.173	2.4	0.62	1.49
6		270	310	0.148	4.6	0.53	2.44
7	3.765	250	280	0.120	2.2	0.49	1.10
8		280	310	0.107	3.0	0.44	1.32
9		310	330	0.064	0.2	0.26	0.05

**Empirical formulas (Ghosh and Mallik 2004; Bansal and Brar 2015)

Figure 11 is the plot showing effort and power vs. percentage change in speed for a Proell governor.

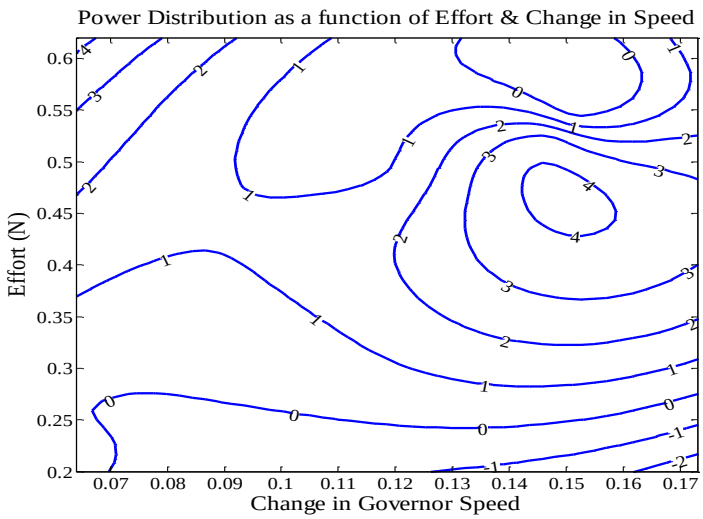

Figure 11: Effort and Power versus percentage change in speed plot of Proell governor.

2.3 Hartnell Governor Set-up

The universal governor set-up is arranged as a Hartnell governor with a spring which is a spring-controlled governor as shown in Fig. 3 driven by a small electric motor with belt and pulley arrangement. Motor and test set up are mounted on a mild steel fabricated stand. The governor spindle is driven by a motor through V-belt and is supported in a ball bearing.

Drive: D.C. motor H.P. = 0.25; speed = 1500 rpm with a speed variation arrangement. Tachometer service required: Earthed A.C. single phase electrical supply 200/250 V, 50/60Hz. After making proper connection with the motor, the speed of motor is gradually increased and speed of spindle is measured with a tachometer and sleeve displacement by the scale provided for three different loads given to the sleeve. The radius of rotation, '*r*' (Khurmi and Gupta 2005) at any position of sleeve is given by,

$$r = r_o + \frac{a}{b} S_m \quad (15)$$

Where r_o is the initial radius of rotation, *'a'* (=7cm) is ball arm length and *'b'*

(=17.5cm) is sleeve arm length of bell-crank lever of the Hartnell governor. The all equations from Eq. (1) to (15) are referred from books listed in reference.

Sleeve displacements were observed for 2.765 kg sleeve load, 3.265 kg load and 3.765 kg load with speed range 130 rpm to 240 rpm (11 readings), 140 rpm to 225 rpm (8 readings) and 250 rpm to 340 rpm (3 readings) respectively as listed in Table 4

Table 4: Governor Speed vs. Sleeve Displacement, Radius of Rotation, and Controlling Force.

	Sl. No	Speed, N (RPM)	Sleeve Displacement, S_m (cm)	Radius of Rotation, r (cm)	Controlling Force, $F=\frac{w}{g}\omega^2 r$ (Newton)
For Sleeve weight, W=2.765kg	1	130	0.1	13.04	8.46
	2	140	0.5	13.22	9.95
	3	150	1.4	13.62	11.76
	4	160	1.5	13.66	13.42
	5	165	1.8	13.79	14.41
	6	180	2.3	14.01	17.42
	7	190	2.5	14.10	19.54
	8	200	2.9	14.28	21.92
	9	215	3.1	14.37	25.50
	10	220	3.4	14.50	26.94
	11	240	3.6	14.59	32.26
Sleeve weight, W=3.265kg					
	1	140	0.05	13.02	9.79
	2	145	0.08	13.04	10.52
	3	170	0.1	13.05	14.48
	4	200	0.6	13.26	20.36
	5	205	0.8	13.35	21.53

	6	210	1.0	13.44	22.75
	7	220	1.7	13.75	25.54
	8	225	1.9	13.84	26.89
Sleeve weight, W=3.765kg					
	1	250	0.8	13.35	32.02
	2	280	0.9	13.40	40.32
	3	340	1.4	13.62	60.42

The results have been plotted graphically as shown in Fig. 12(a) and Fig. 12(b) for performance analysis. The reason for selecting only three readings during sleeve load 3.765 kg is to observe the performance beyond 340 rpm and further increase in speed is not possible due to limitation of sleeve displacement by upper stop mounted on the spindle.

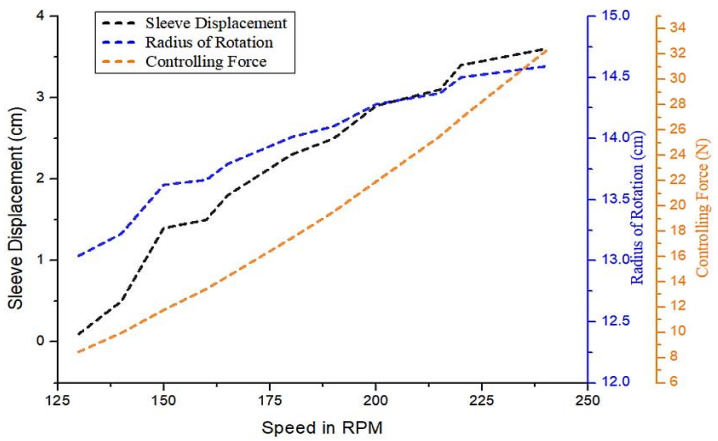

Figure 12 (a): Speed versus sleeve displacement, radius of rotation and controlling force plot for 2.765 kg sleeve load.

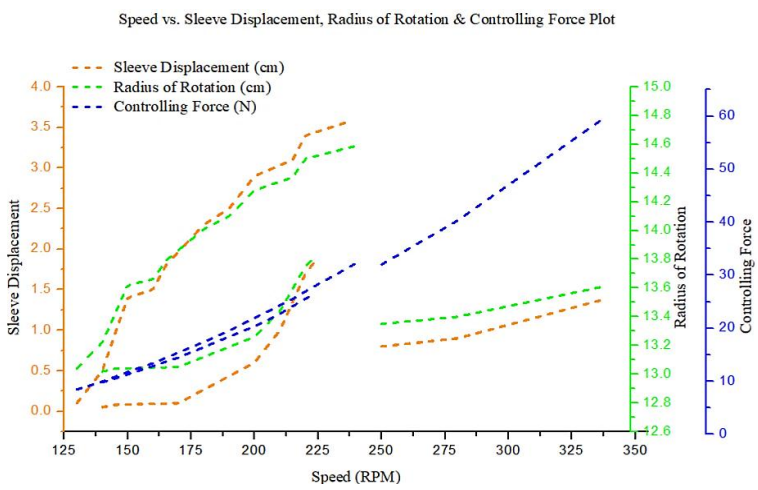

Figure 12 (b): Speed versus sleeve displacements, radius of rotation and controlling force plots for 2.765kg, 3.265kg and 3.765 kg sleeve load.

Again, the controlling force curve of Hartnell governor may be drawn by taking radius of rotation in abscissa and controlling force in primary ordinate and speed in rpm in secondary ordinate. Figure 13 shows the controlling force curve for 2.765 kg, 3.265 kg and 3.765 kg sleeve load.

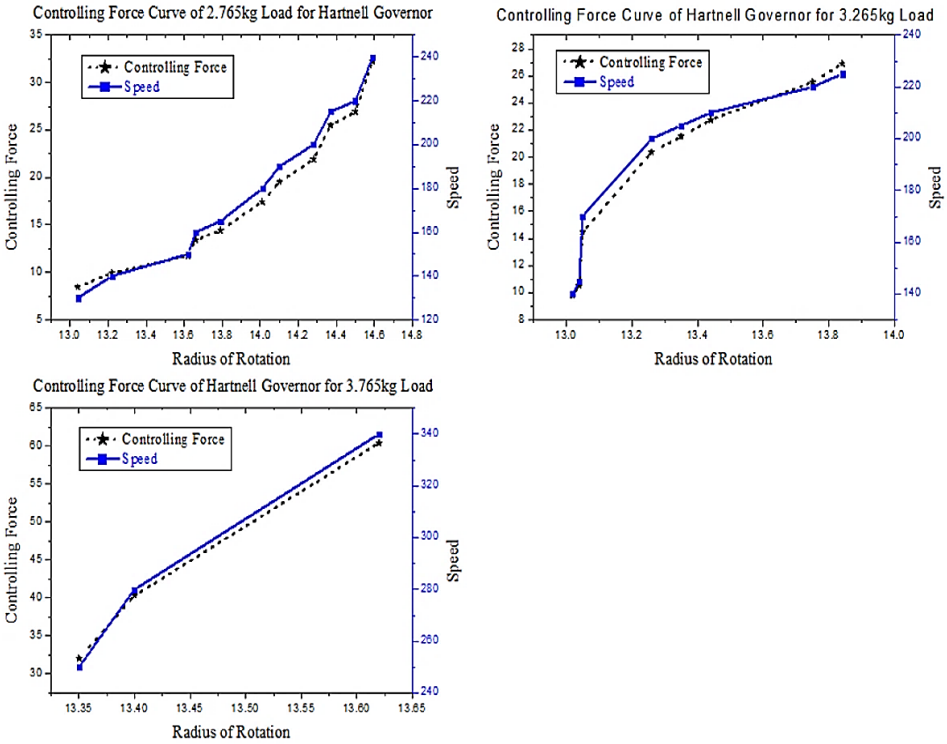

Figure 13: Controlling Force Curve of Hartnell Governor for 2.765 kg, 3.265 kg and 3.765 kg Sleeve Load.

Effort and Power of Hartnell governor with percentage change in speed are listed in Table 5.

****Table 5. Effort and Power against Percentage change in speed of Hartnell governor.**

Sl. No.	Weight of Sleeve, W (kg)	Minimum Spring Force, S_1 (N)	Maximum Spring Force, S_2 (N)	Initial Speed, N_1 (rpm)	Final Speed, N_2 (rpm)	Percentage Change in Speed, $C=\frac{N_2-N_1}{N_1}$	Lift of Sleeve, S_m (cm)	Effort= $C\left(W+\frac{S_1+S_2}{2}\right)$ (N)	Power = Effort × Lift of Sleeve (watt)
1	2.765	38.35	302.74	130	160	0.23	1.40	40	56
2				160	190	0.19	1.00	33	33
3				190	220	0.16	0.90	28	25.2
4	3.265	44.34	227.1	140	200	0.43	0.60	60	36
5				200	210	0.05	0.40	7	2.8
6				210	220	0.047	0.42	6.5	2.73
7	3.765	145.25	192.48	250	260	0.04	0.10	7	0.7
8				260	285	0.096	0.50	16.57	8.3
9				270	290	0.07	0.58	12	7.0

**Empirical Formulas (Ballaney 2014; Shigley, Pennock, and Uicker 2014)

Graphical representations of the above results are plotted in Fig. 14 to visualize the variations at three different loads.

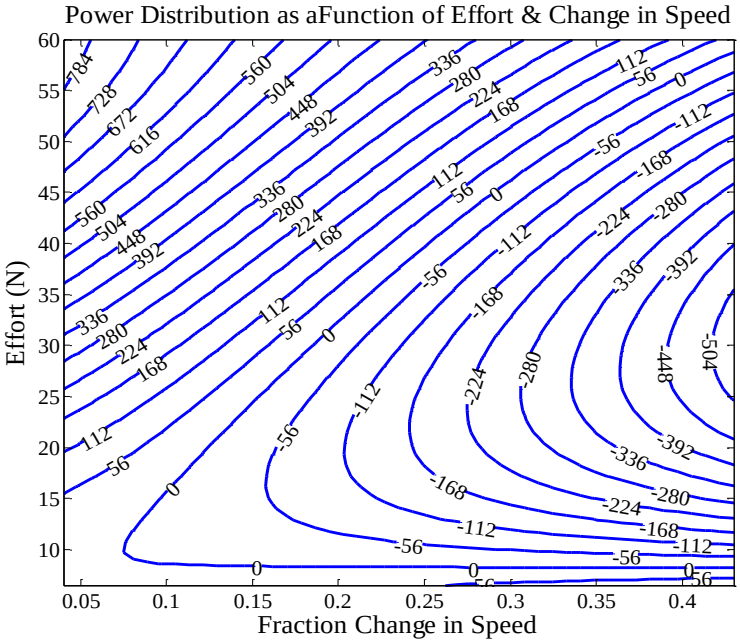

Figure 14: Effort and power versus percentage change in speed plot of Hartnell governor.

Sensitivity of each type of governor i.e., Porter, Proell and Hartnell governor is determined on the basis of minimum and maximum equilibrium speed against 2.765 kg, 3.265 kg and 3.765 kg sleeve loads are shown in Table 6.

****Table 6: Sensitivity of Porter, Proell and Hartnell Governor vs. Sleeve Load.**

	Sl No	Load given on sleeve (kg)	Minimum equilibrium speed (N_1)	Maximum equilibrium speed (N_2)	Range of speed (N_2-N_1)	Mean speed ($\frac{N_1+N_2}{2}$)	Sensitivity = $\frac{Range\ of\ speed}{Mean\ speed}$
Porter Governor	1	2.765	200	550	350	375	0.933
	2	3.265	200	330	130	265	0.490
	3	3.765	240	330	90	285	0.315
Proell Governor	1	2.765	200	380	180	290	0.620
	2	3.265	200	330	130	265	0.490
	3	3.765	240	330	90	285	0.320
Hartnell Governor	1	2.765	130	350	220	240	0.920
	2	3.625	140	300	160	220	0.730
	3	3.765	220	285	65	252.5	0.260

**Empirical Formulas (Bansal and Brar 2015)

Graphically, sensitivity of the three types of governors against three different sleeve loads are shown in Fig. 15.

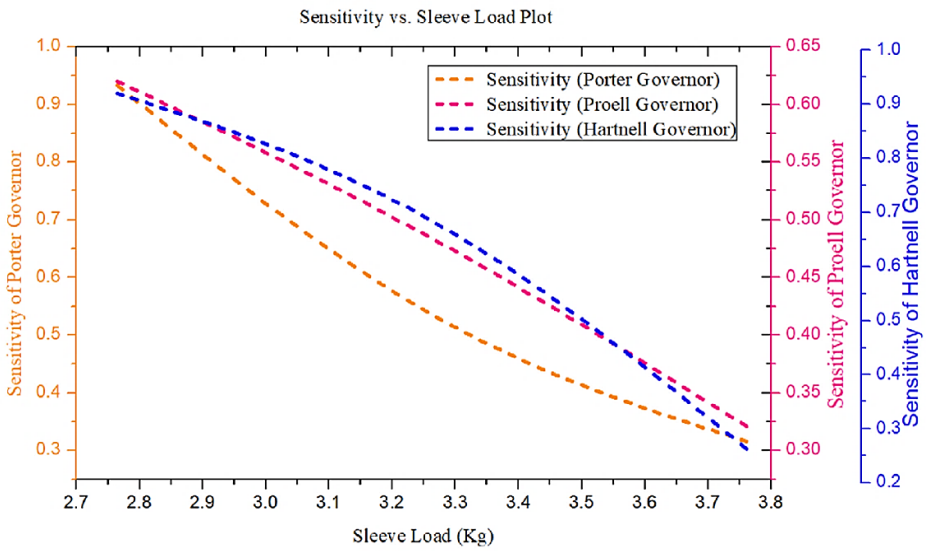

Figure 15: Sensitivity versus Sleeve Loads of Porter, Proell and Hartnell governor.

Figure 16 shows the plot of various spindle speed in RPM vs. sleeve displacement, radius of rotation and controlling force of Porter, Proell and Hartnell governor together at 2.765kg, 3.265kg and 3.765kg sleeve load.

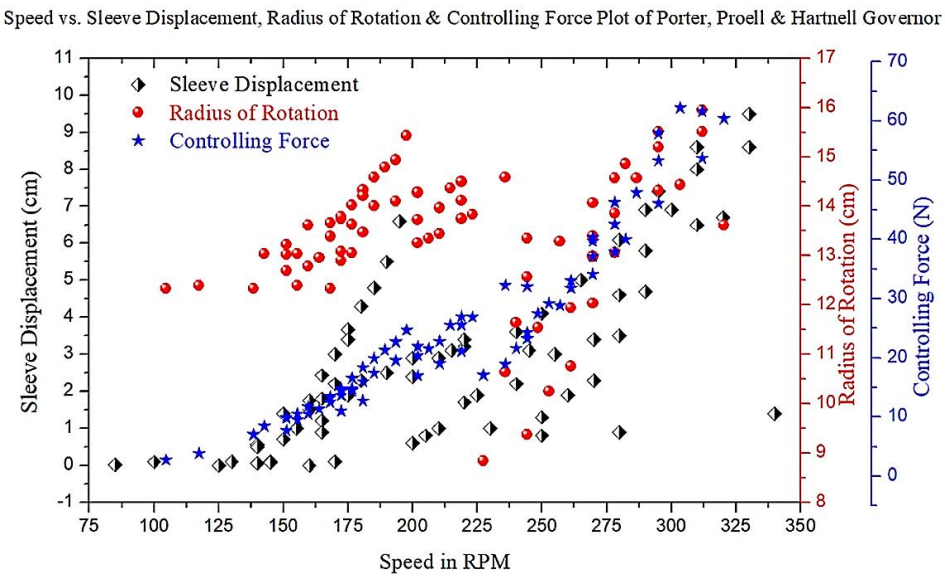

Figure 16: Speed versus Sleeve Displacement, Radius of Rotation and Controlling Force curve for Porter, Proell and Hartnell Governor.

2. RESULTS AND DISCUSSION

Results have already been shown from Fig. 2 to 16 and with Table 1 to 6. Results were initially verified for a porter governor that sleeve displacement increases with increase in speed to check the stability of the instrument and similar is the case of Proell governor in Fig. 8(a). Speed versus sleeve lift, height, controlling force, and radius of rotation curve is showing almost consistency for all the three governors at different sleeve loads. Errors may be accounted for sparking, friction and parallax which may be clearly understood from the effort and power versus percentage change in speed plot of Proell governor (Fig. 11) where power curves, which are product of effort and sleeve displacement is deviated as a result of non-uniformity of sleeve displacements. Controlling force versus sleeve displacement and radius of rotation curves show steeper in nature with increase in sleeve loads. Controlling force depends on load on sleeve. However, controlling force curve is more adequate for lower value 2.765 kg loads out of three randomly selected sleeve loads for porter governor. In case of Proell governor, controlling force is more adequate for 3.265 kg sleeve load as seen from Fig. 10. Similar types of results were followed by a spring controlled Hartnell governor. On the other hand, if we check the sensitivity of the three governors against their sleeve loads from Fig. 15, then one can find that sensitivity curve of Porter and Hartnell governor are mirror image of each other. Again, it has been seen from Fig. 16, that controlling force values of the three governors lies within a particular band width irrespective of radius of rotation and sleeve displacements at different speeds and different sleeve loads. Contrary to that, radius of rotation and sleeve displacements are deviated from mean position with respect to different speed level and sleeve loads.

The verification has been done with best surface fit model (poly 22) for Porter governor and shown in Fig. 17(a).

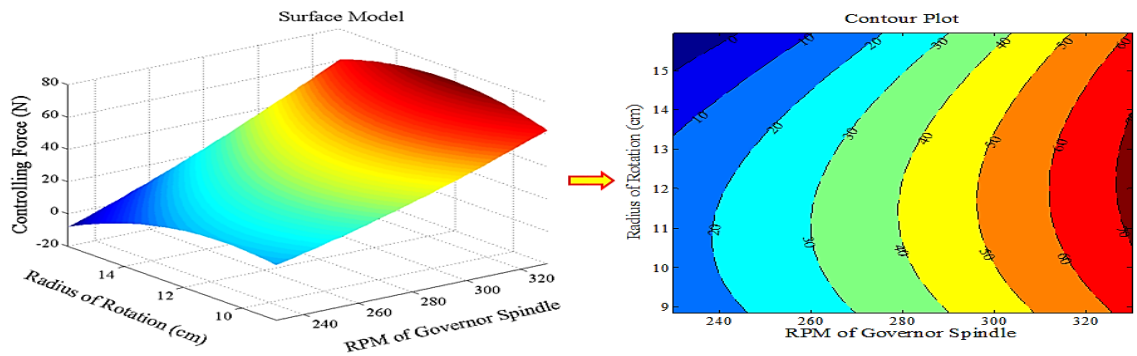

Figure 17(a): Figure shows the surface plot and corresponding contour plot (poly 22) for the results obtained in case of Porter governor.

The controlling force along the Z-axis, is a function of radius of rotation (along X-axis) and RPM of the governor (along the Y-axis).

Similarly, best surface fit model (poly 22) and its corresponding contour plot have been used for verification of results obtained in case of Proell governor in Fig. 17(b).

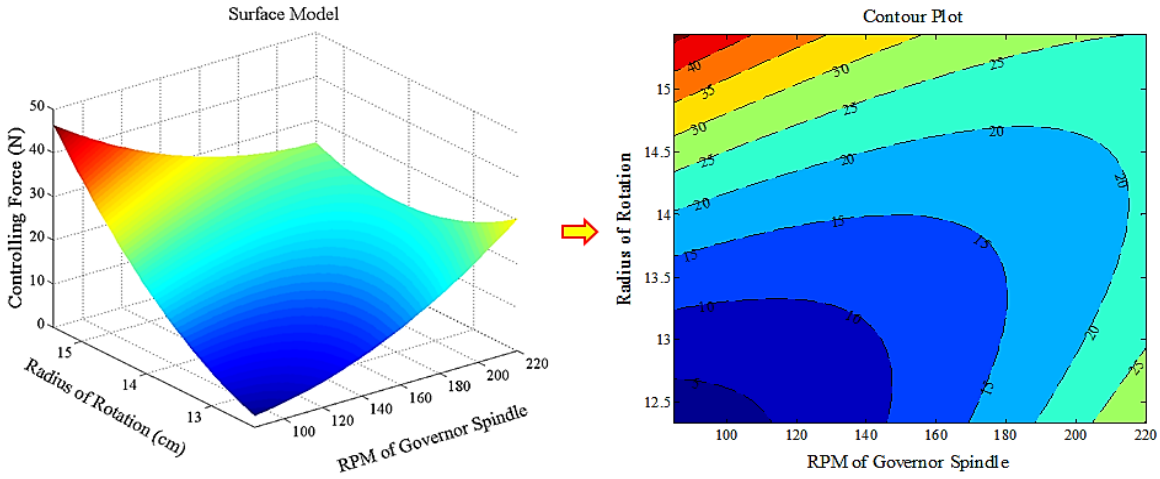

Figure 17(b): Figure shows the surface plot and corresponding contour plot (poly 22) for the results obtained in case of Proell governor.

Again, the verification for Hartnell has been done with best surface fit model poly 12, using MATLAB and shown in Fig. 17(c).

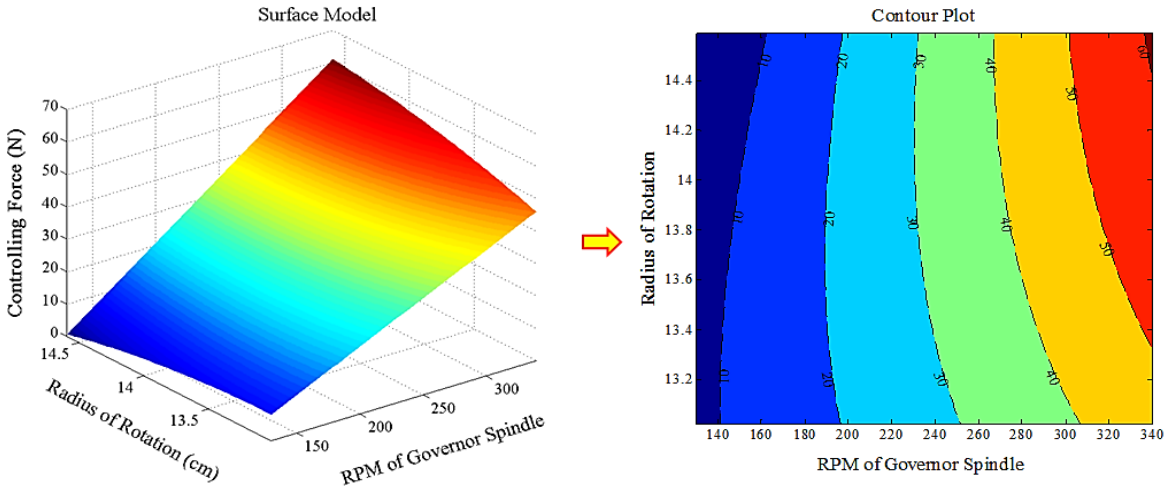

Figure 17(c): Figure shows the surface plot and corresponding contour plot (poly 12) for the results obtained in case of Hartnell governor.

3. CONCLUSION

It is concluded from controlling force curve that Porter governor performance is smooth at lower sleeve load and that for Hartnell governor is at comparatively higher value. Proell governor shows in between these two. The mirror image sensitivity behaviour of Porter and Hartnell governor may be a field of study where one can see the extreme two opposite nodes at 3.265 kg sleeve load. Diagnostic and prognostic may be done in vibration analysis of the governor for better performance in application. Since all the plots verify the stability condition of the three governors, due to higher sensitivity, Hartnell governor is recognised as best among three and may have replacement in old heavy diesel engine, as well as turbine and carburettor used petrol engine for better fuel economy and reliability purpose. Figure 18 shows replacement of Hartnell governor in a diesel engine,

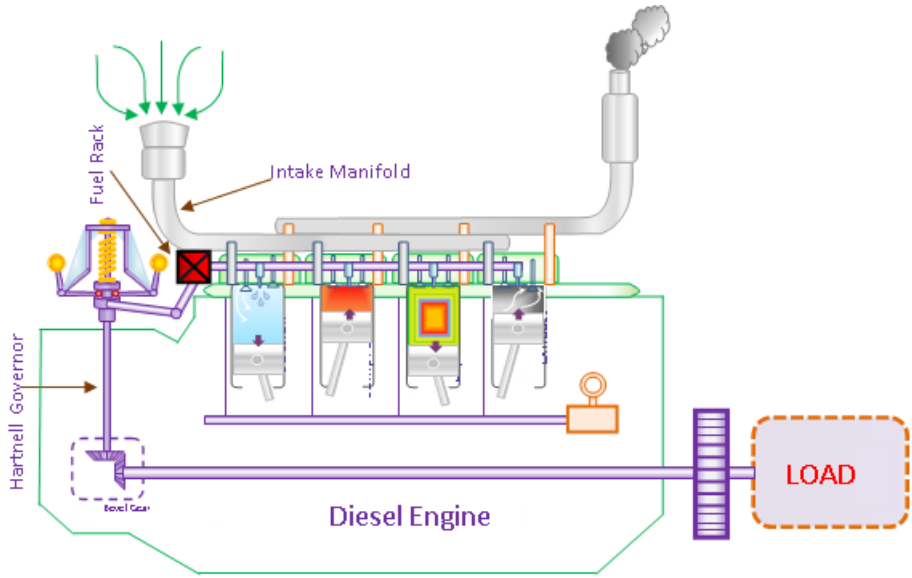

Figure 18: Application of speed control Hartnell governor in diesel engine.

4. ACKNOWLEDGEMENT

We acknowledge to Mechanical Engineering Department and staff members of mechanical engineering laboratory of Jorhat Engineering College, Jorhat-785007, who directly or indirectly help us to complete the project.

5. Nomenclature

a = ball arm length

b = sleeve arm length

c = percentage change in speed

d = differential operator

E = energy capacity of governor

F = controlling force

h = height of governor

h_o = initial height of governor

L = arm length

M = mass of sleeve

m = mass of fly ball

N = governor equilibrium speed in rpm.

$N_{1,2}$ = minimum and maximum

P = effort of governor

equilibrium speed of governor

r = radius of governor

S_m= sleeve displacement

α = angle of inclination of upper link

$S_{1,2}$ = minimum and maximum spring

ω = angular speed of governor spindle force in Hartnell governor

β = angle of inclination of lower link

ORCID

Debarupam Gogoi https://orcid.org/0000-0002-1503-8605

REFERENCES

1. Pranaby, J., B. Porter. Non-linear vibrations of a centrifugal governor. *International Journal of Mechanical Sciences*, 1968; 10(3): 187-200. doi:10.1016/0020-7403(68)90078-7.
2. Kogiso, k., K. Hirata. Reference governor for constrained systems with time- varying references. *Journal of Robotics and Autonomous System*, 2009; 57(3): 289-295. doi:10.1016/j.robot.2008.10.015.
3. Nakada, H., P. Martin, A. Wijesinghe, H. Shirai, A. Matsunaga, H. Tominaga. An application of reference governor to a diesel engine air path system: Implementation of a multi-variable reference modification algorithm. *Journal of IFAC-PapersOnLine*, 2016; 49(11): 582-588. doi:10.1016/j.ifacol.2016.08.085.
4. WANG, j., H. WANG, L. GUO. Anti-control of chaos in mechanical centrifugal governor system. *Journal of Information & Computational Science*, 2012; 9(17): 5127–5133.

5. Mello, L. F., J. Sotomayor, D. d. C. Braga. Stability and hopf bifurcation in the watt governor system. *Journal of Communications on Applied Nonlinear Analysis*, 2006. ISSN: 1074-133X. https://arxiv.org/abs/math/0604177v1.
6. Cheng, J., H. Xu. Periodic motions, bifurcation, and hysteresis of the vibro-impact system. *Journal of Mechanics Based Design of Structures and Machines*, 2007; 35(2): 179-203. doi: 10.1080/15397730701291404.
7. Ge, Z.-M., H.-S. Yang, H.-H. Chen, H.-K. Chen. Regular and chaotic dynamics of a rotational machine with a centrifugal governor. *International Journal of Engineering Science*, 1999; (37): 921-943. doi: 10.1016/S0020-7225(98)00092-5.
8. Lengyel, A., Z. You. Analogy between bifurcations in stability of structures and kinematics of mechanisms. *Journal of Mechanics Based Design of Structures and Machines*, 2006; 31(4): 491-507. doi: 10.1081/SME-120023168.
9. Miljic, N. L., S. J. Popovic. Model based tuning of a variable-speed governor for a distributor fuel-injection pump. *Journal of FME Transactions*, 2014; 42(1): 40-48. doi: 10.5937/fmet1401040M.
10. Yunpu, S., S. Yixing. Design of structural parameters for centrifugal elevator over-speed governors. *Journal of Sensors & Transducers*, 2014; 163(1): 171-179. e-ISSN 1726-5479.
11. Manhotra, S. K. Design & validation of e-rpm adjustment assembly for mechanical governor system. *International Journal of Scientific & Technology Research*, 2017; 6(11): 266-269. ISSN 2277-8616.
12. Navathale, T. J., A. A. Paralkar, V. S. Ghorade. Design and analysis of centrifugal governor: A review. *International Research Journal of Engineering and Technology*, 2017; 04(01): 1058-1062. e-ISSN: 2395 -0056.
13. Rao, X.-B., Y.-D. Chu, L. -Xu, Y. –X. Chang, J. –G. Zhang. Fractal structures in centrifugal flywheel governor system. *Journal of Communications in Nonlinear Science and Numerical Simulation*, 2017; 50: 330-339. doi:10.1016/j.cnsns.2017.03.016.
14. Rao, X. –B., Y. –D. Chu, Y. –X. Chang, J. –G. Zhang. Broken farey tree and fractal in a hexagonal centrifugal governor with a spring. *Journal of Chao, Solutions & Fractals*, 2018; 107: 251-255; doi:10.1016/j.chaos.2018.01.015.
15. Ge, Z. –M., C. –I. Lee. Anticontrol and synchronization of chaos for an autonomous rotational machine system with a hexagonal centrifugal governor. *Journal of Sound and Vibration*, 2005; 282(3-5): 635-648. doi: 10.1016/ j.jsv.2004.03.034.

16. Sotomayor, J., L. F. Mello, D. d. C. Braga. Stability and hopf bifurcation in a hexagonal governor system. *Journal of Nonlinear Analysis: Real World Applications*, 2008; 9(3): 889-898. doi: 10.1016/j.nonrwa.2007.01.007.
17. Dems, K., R. K. Haftka. Two Approaches to Sensitivity Analysis for Shape Variation of Structures. *Journal of Mechanics of Structures and Machines*, 2007; 16(4): 501-522. doi: 10.1080/08905458808960274.
18. Rattan, S.S. *Theory of machines* New Delhi: Tata McGraw Hill Education Private Limited, 2011; 3.
19. Khurmi, RS., and J. K. Gupta. *Theory of machines*. New Delhi: S. Chand, 2005; 14.
20. Thomas, B. *Theory of machines*. 3rd ed. Chennai: Pearson Education India, 2009.
21. Rao, J. S., and R. V. Dukkipati. *Mechanism and machine theory*. New Delhi: New Age International Publishers, 2014; 2.
22. Ghosh, A., and A. K. Mallik. *Theory of mechanisms and machines*. New Delhi: EWP Private Limited, 2004; 1.
23. Bansal, R. K., and J. S. Brar. *Theory of machines*. New Delhi: Laxmi Publications, 2015; 5.
24. Ballaney, P. L. *Theory of machines and mechanisms*. New Delhi: Khanna Publishers, 2014; 25.
25. Shigley, J. E., G. R. Pennock, and J. J. Uicker. *Theory of machines and mechanisms.* Oxford University Press, 2014; 4.